

Cellular dynamical mean-field theory of the periodic Anderson model

Lorenzo De Leo,¹ Marcello Civelli,² and Gabriel Kotliar¹

¹*Department of Physics and Center for Material Theory, Rutgers University, Piscataway, New Jersey 08854, USA*

²*Institut Laue Langevin, 6 rue Jules Horowitz, 38042 Grenoble, Cedex, France*

(Received 20 February 2007; revised manuscript received 12 September 2007; published 8 February 2008)

We develop a cluster dynamical mean-field theory of the periodic Anderson model in three dimensions, taking a cluster of two sites as a basic reference frame. The mean-field theory displays the basic features of the Doniach phase diagram: a paramagnetic Fermi liquid state, an antiferromagnetic state, and a transition between them. In contrast with spin-density wave theories, the transition is accompanied by a large increase of the effective mass everywhere on the Fermi surface and a substantial change of the Fermi surface shape across the transition. To understand the nature and the origin of the phases near the transition, we investigate the paramagnetic solution underlying the antiferromagnetic state, and identify the transition as a point where the f electrons decouple from the conduction electrons undergoing an orbitally selective Mott transition. This point turns out to be intimately related to the two-impurity Kondo model quantum critical point. In this regime, nonlocal correlations become important and result in significant changes in the photoemission spectra and the de Haas-van Alphen frequencies. The transition involves considerable f spectral weight transfer from the Fermi level to its immediate vicinity, rather than to the Hubbard bands as in single-site dynamical mean-field theory.

DOI: [10.1103/PhysRevB.77.075107](https://doi.org/10.1103/PhysRevB.77.075107)

PACS number(s): 71.27.+a, 71.10.Hf, 75.20.Hr, 75.30.Mb

I. INTRODUCTION

The heavy fermion materials have been one of the most challenging problems for the condensed matter community in the past three decades. The physics of these systems is dominated by the competition of many interactions, manifesting in a variety of phases.¹ Close to the zero-temperature transition between two such phases the materials typically show non-Fermi liquid behavior on a large temperature range. This behavior has been often attributed to an underlying quantum critical point (QCP).

In a subclass of these materials (including $\text{CeCu}_{6-x}\text{Au}_x$, YbRh_2Si_2 , and CeTIn_5 , with $T=\text{Ir, Co, Rh}$) it is possible to drive the system from an antiferromagnetic (AF) phase to a paramagnetic (PM) phase by suppressing continuously the Néel temperature via application of pressure, magnetic field, or doping. The conventional spin-density wave (SDW) theory of a QCP²⁻⁴ disagrees with the experimental evidence in many of these materials.^{1,5-8} This has triggered a renewed interest in microscopic descriptions of the heavy fermion state and its possible instabilities to ordered states. More generally, not only the critical point but also the formation of the heavy fermion state in the regime where the Ruderman-Kittel-Kasuya-Yosida (RKKY) interactions are sizable requires nontrivial techniques for its microscopic description.^{9,10} Heavy fermion materials can be modeled by the periodic Anderson model which describes a wide conduction band of spd electrons and a narrow band of f electrons which is strongly correlated and hybridized with the spd electrons.

Doniach¹¹ established that for large hybridization the f electrons combine with the conduction electrons to form a heavy Fermi liquid, while for small hybridization the f moments order magnetically and hence do not undergo the Kondo effect. Thus, changes in the hybridization not only lead to the appearance of magnetic long-range order but in-

troduce also a change in the electronic structure referred to as f - c decoupling or Kondo breakdown (KB). Namely, for large values of the hybridization the quasiparticles are composites of f electrons and conduction c electrons with a Fermi surface which obeys Luttinger theorem, counting both the f and c electrons. For small hybridization the f electrons decouple from the conduction electron quasiparticles, and the Fermi surface contains only the latter. The decoupling between the f and c electrons can be viewed as an orbitally selective Mott transition, and has been studied with single-site dynamical mean-field theory (DMFT)¹² and slave boson techniques.¹³ As stressed in Ref. 14, a precise formulation of KB requires the elimination of antiferromagnetic long-range order which breaks the translational symmetry of the original lattice. So far this has been achieved by studying models with disorder within DMFT,¹⁵ or by modifying the symmetry group of the spin from $\text{SU}(2)$ to $\text{SU}(N)$.¹⁴ For earlier studies of the KB using slave bosons, see Refs. 16 and 17.

Single-site extended DMFT of various models has been carried out. For the Anderson lattice model,^{18,19} the KB and the onset of AF should be viewed as distinct instabilities which occur at two different values of the RKKY coupling (relative to the Kondo coupling). The same situation occurs in the field theory approach of Ref. 14.

On the other hand, extended DMFT studies of a Kondo lattice model, in which the conduction electron band is constrained so as to prevent its magnetic polarization, reveal that the KB and the onset of magnetism take place at the same point in the phase diagram.²⁰⁻²³ See, however, Ref. 24. Justification for the study of this model is given in Ref. 25.

In DMFT based approaches the breakdown of Fermi liquid theory at the transition is understood in terms of local physics. In other works the same breakdown is explained in terms of the coupling of the electrons to the long wavelength fluctuations of an emergent gauge field¹⁴ and to the Kondo order parameter fluctuations.^{13,26}

In this paper we handle the competition between magnetism and formation of a heavy PM state in an unbiased way using cellular dynamical mean field theory (CDMFT).²⁷ This approach improves the treatment of nonlocal correlations over single-site DMFT considering a cluster of sites and providing a self-consistency condition on the cluster action. All the correlations whose range is contained within the cluster are then treated beyond a simple mean-field level. In this paper we consider a cluster of two sites embedded in a three-dimensional lattice, which is the minimal unit able to capture the competition between PM and AF correlations. A similar approach was introduced in an earlier publication¹⁰ based on a quantum Monte Carlo impurity solver, but that study was limited to large temperatures and small values of U . We overcome this limitation by using exact diagonalization (ED) as an impurity solver.²⁸ This solver gives access to the ground state properties of the system with a finite energy resolution (typically 0.005 of the bandwidth in our case).

In the theory of the Mott transition, the investigation of the PM insulating phase has been very fruitful and allowed an understanding of the finite temperature state, above the magnetic order in many compounds. We pursue a similar approach to the periodic Anderson model by investigating both the magnetic and a “parent compound” PM state, to understand better the character of the electronic structure. This allows us to describe the magnetic state as a result of an additional instability of the PM state.

We show that a phase transition separates the heavy fermion paramagnetic phase from an antiferromagnetic phase. Approaching the transition from the paramagnetic side the Fermi liquid is strongly renormalized. An analysis of the mean-field PM solution into the AF phase reveals an orbitally selective Mott decoupling and localization of the f electrons. Within the resolution of our method, the antiferromagnetic transition and the decoupling of the f and c electrons take place for the same value of the hybridization. Through a comparison with a Wilson’s numerical renormalization group (NRG) calculation, we further relate the nature of the transition to the proximity of the system in the parameter space to the quantum critical point of the two-impurity Kondo model (2IKM).^{29,30}

The transition has dramatic consequences on the quasiparticle spectra and on the topology of the Fermi surface which can be detected by photoemission experiments and by Hall effect and de Haas–van Alphen frequency measures.

The paper is organized as follows. In Sec. II we introduce the model Hamiltonian and the CDMFT method employed. In Sec. III we analyze the results of the CDMFT calculations and compare them with single-site DMFT results and numerical renormalization group results on the underlying impurity problem. Conclusions are presented in Sec. IV.

II. METHODS

The three-dimensional periodic Anderson model Hamiltonian is

$$H = -t \sum_{\langle ij \rangle} c_{i\sigma}^\dagger c_{j\sigma} - \mu \sum_i c_{i\sigma}^\dagger c_{i\sigma} + V \sum_i (f_{i\sigma}^\dagger c_{i\sigma} + \text{H.c.}) + (E_f - \mu) \sum_i f_{i\sigma}^\dagger f_{i\sigma} + U \sum_i n_{i\uparrow}^f n_{i\downarrow}^f, \quad (1)$$

where $c_{i\sigma}^\dagger$ creates a conduction band electron at site i with

spin σ and $f_{i\sigma}^\dagger$ does the same for the localized orbitals. The conduction electron bandwidth $W=12|t|=2$ sets the energy unit.

In the large U/V limit the model maps onto the Kondo lattice model, where each f orbital is replaced by a spin $\frac{1}{2}$ which is Kondo coupled to the local conduction electrons with a coupling $J_K = \left(\frac{1}{|E_f - \mu|} + \frac{1}{|U + E_f - \mu|} \right) V^2$, where ρ is the conduction electron density of states at the chemical potential. It is also possible to define two energy scales in the problem. The first is the single-impurity Kondo temperature $T_0 = \exp(-1/2\rho J_K)$. It is not known *a priori* how the “lattice” Kondo energy is related to T_0 . The second scale is set by the magnetic interactions. These are not contained explicitly in this Hamiltonian, but an effective RKKY coupling is generated in fourth order perturbation theory in V (second order in the Kondo coupling, $J_{RKKY} \sim J_K^2/W$). The RKKY coupling oscillates in real space with a period that is related to the bare conduction band Fermi momentum, ranging from antiferromagnetic at half-filling to ferromagnetic in the limit of an empty band. A comparison of these two energy scales allows us to understand the qualitative features of the phase diagram of the model.¹¹ The ratio between Kondo temperature and RKKY interaction is an increasing function of V , hence for small V we will find a phase in which the magnetic fluctuations dominate giving rise to an ordered state, while for large V the Kondo effect dominates and the f moments are screened by the conduction electrons.

At half-filling the Kondo screening of the moments by the conduction electrons results in an insulator with a gap induced by the hybridization. In this paper we are interested in metallic heavy fermions, and we restrict ourselves to study the system away from half-filling.

In the path integral formalism the conduction band can be integrated out in the action and replaced by an effective long-range retarded hopping for f electrons. After these manipulations the Lagrangian of the system is

$$\mathcal{L} = \sum_i f_{i\sigma}^\dagger(\tau) (\partial_\tau - \mu + E_f) f_{i\sigma}(\tau) + \sum_{ij} f_{i\sigma}^\dagger(\tau) \Delta_{ij}^c(\tau - \tau') f_{j\sigma}(\tau') + U \sum_i n_{i\uparrow}^f n_{i\downarrow}^f, \quad (2)$$

where the effect of the conduction band is absorbed in the Weiss field

$$\Delta^c(i\omega, \mathbf{q}) = \frac{V^2}{i\omega + \mu - \varepsilon_{\mathbf{q}}} \quad (3)$$

and $\varepsilon_{\mathbf{q}} = -2t \sum_{a=x,y,z} \cos(q_a)$.

In CDMFT the original three-dimensional lattice is now tiled with a superlattice of clusters and an effective Anderson impurity action is derived for a single cluster. Finally a self-consistency condition relates the cluster Green’s function to the local Green’s function of the superlattice. The self-consistency is more easily written as a matrix form

$$G_{loc}(i\omega) = \sum_{\vec{k}} \left[\begin{pmatrix} i\omega + \mu - E_f & 0 \\ 0 & i\omega + \mu - E_f \end{pmatrix} - \frac{V^2}{(i\omega + \mu)^2 - \varepsilon_{\vec{k}}^2} \begin{pmatrix} i\omega + \mu & e^{ik_x \varepsilon_{\vec{k}}} \\ e^{-ik_x \varepsilon_{\vec{k}}} & i\omega + \mu \end{pmatrix} - \begin{pmatrix} \Sigma_{11}(i\omega) & \Sigma_{12}(i\omega) \\ \Sigma_{21}(i\omega) & \Sigma_{22}(i\omega) \end{pmatrix} \right]^{-1}, \quad (4)$$

where spin index has been suppressed to simplify the notation. It is very important to notice that in the large U/V limit the impurity action becomes equivalent to the action of a two-impurity Kondo model away from particle-hole (p - h) symmetry. At p - h symmetry this model is known to have a QCP separating a Kondo screened phase from a phase in which the impurities are decoupled from the conduction band.^{29,30} Away from p - h symmetry the QCP is not accessible but still influences the physics in an intermediate energy range.^{31,32}

In order to solve the cluster-impurity problem we employ ED. In this method the cluster action is recast in the form of an Anderson impurity Hamiltonian where the continuous degrees of freedom of the free electron bath are parametrized by a finite number N_b of sites as follows:

$$H_{ED} = \sum_{i=1,2} f_{i\sigma}^\dagger (E_f - \mu) f_{i\sigma} + U \sum_{i=1,2} n_{i\uparrow}^f n_{i\downarrow}^f + \sum_{l=1, N_b} \varepsilon_{l\sigma} a_{l\sigma}^\dagger a_{l\sigma} + \sum_{i,l} (V_{il\sigma} a_{l\sigma}^\dagger f_{i\sigma} + \text{H.c.}). \quad (5)$$

In this representation the hybridization function $\Delta_{\mu\nu} = \mathcal{G}_{\mu\nu}^0 - (i\omega + \mu - E_f) \delta_{\mu\nu}$, related to the noninteracting impurity Green's function $\mathcal{G}_{\mu\nu}^0 = -\langle f_{\mu} f_{\nu}^\dagger \rangle_{U=0}$ of the cluster-impurity problem, becomes

$$\Delta_{ij\sigma}(i\omega) = \sum_{l=1, N_b} \frac{V_{il\sigma}^* V_{jl\sigma}}{i\omega - \varepsilon_{l\sigma}}, \quad (6)$$

where the indices $i, j=1, 2$ represent the cluster sites. In the figures presented in this work we used eight sites in the bath, but the results have been tested in a few points using ten sites.

The ground state and Green's functions of this Hamiltonian are determined via the Lanczos procedure and the self-consistency equation in turn allows us to derive a new set of bath parameters. The self-consistency condition is used to determine the Δ function on a finite mesh of points $\omega_n = (2n+1)\pi/\beta$. This implies a finite resolution in frequency. We used $\beta=100$. The process is iterated until convergence is reached. To study the interplay of antiferromagnetism and Kondo screening we restrict the study to the metallic regime close to half-filling where the RKKY interaction is predominantly antiferromagnetic. This is achieved by fixing the values $U=10$, $E_f=-5.5$, and $\mu=0.2$ throughout the paper. Being a mean-field theory, DMFT gives the possibility to selectively allow some instabilities and forbid others. Thus we will allow the development of AF order and study the realistic material phase diagram. However, we will also force the

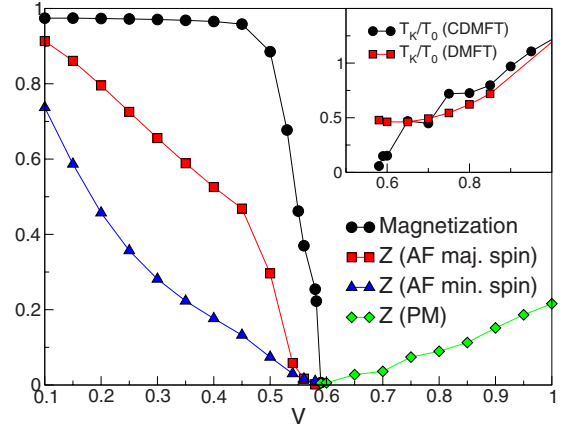


FIG. 1. (Color online) Magnetization M and average of the quasiparticle residue Z eigenvalues for the AF (both for majority and minority spin) and PM solutions as a function of V . Inset: ratio between lattice and single-impurity Kondo energies in DMFT and CDMFT.

system to remain in a PM state to study the “normal state” underlying the AF phase. This will prove important to study the KB point and to understand the origin of the transitions in the system.

III. RESULTS

We compute the staggered magnetization $M = \langle n_{1\uparrow}^f \rangle - \langle n_{1\downarrow}^f \rangle = -(\langle n_{2\uparrow}^f \rangle - \langle n_{2\downarrow}^f \rangle)$ as a function of V (Fig. 1). For small V the RKKY interaction is dominating and the solution describes an AF state with a magnetization close to one. In the opposite limit of large V , where the Kondo screening is more effective, the system is a PM metal. Increasing V in the AF phase, the magnetization decreases smoothly and approaches zero at a value $V^* \sim 0.585$ where a phase transition occurs. Above this critical value the system becomes paramagnetic. The value of M at the transition jumps from ~ 0.22 for $V = 0.58$ to ~ 0.006 for $V = 0.59$ and in between the convergence becomes extremely slow. The numerical accuracy does not allow us to exclude a weakly first order transition scenario, although in this case the coexistence region would be very small.

To clarify the nature of the transition we investigate the cluster quasiparticle residue $\hat{Z} = (\hat{1} - \partial \hat{\Sigma} / \partial \omega)^{-1}|_{\omega=0}$ (in this case, a matrix in spin and cluster indices). The AF three-dimensional SDW theory predicts that antiferromagnetism develops from a well defined Fermi liquid state and hence a finite quasiparticle residue Z at the transition. On the contrary KB scenarios predict that Z goes to zero at the transition. In Fig. 1 we plot the \hat{Z} eigenvalues. In the AF phase the two curves correspond to minority and majority species. In the PM phase we plot only the average of the eigenvalues since the difference is not appreciable on the scale of the plot. In both phases the eigenvalues of the \hat{Z} matrix decrease as we approach the transition. Precisely at the transition one eigenvalue goes to zero, suggesting that the KB is indeed the correct scenario in this model.

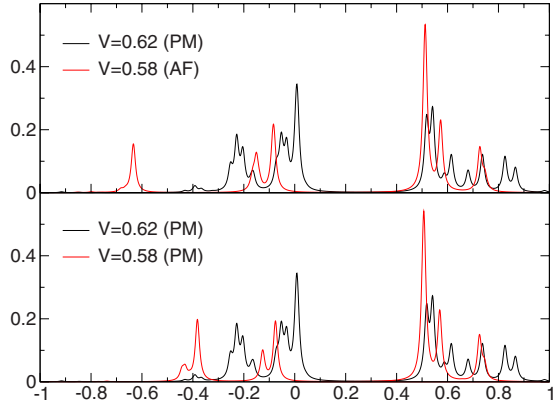


FIG. 2. (Color online) Spectral function of the f electrons on the two sides of the transition with AF order allowed (upper panel) and forbidden (lower panel). The two Hubbard bands are outside the energy range.

Approaching the transition from the PM phase by reducing V , we observe a strong reduction of the \hat{Z} eigenvalues leading to a large effective mass enhancement. This result suggests that increasing the correlations by decreasing V from the PM side, the Fermi liquid becomes heavier and heavier, and eventually it is more favorable to get rid of the entropy by developing AF long-range order. The fundamental difference with the SDW picture is that here the mechanism responsible for the instability is short ranged in space. The cluster self-energies are, in fact, approximately local on the PM side of the transition. This may lead to think that the results are essentially similar to a single-site DMFT solution of the periodic Anderson model. However, there are essential differences. Indeed, even setting the off-diagonal self-energy $\hat{\Sigma}_{12}=0$ the CDMFT self-consistency equations do not reduce to the corresponding single-site DMFT equations. To demonstrate this we compare in the inset of Fig. 1 the ratio between the lattice Kondo temperature obtained through the relation $T_K=\Delta(0)Z$ and the corresponding single-impurity energy T_0 in the two cases. While the DMFT result gives a smooth and finite T_K across V^* , in CDMFT T_K appears to approach a zero value at the transition.

We take advantage now of the possibility of suppressing the AF long-range order to study the normal PM solution in the AF phase. For $V < V^*$ this solution is obviously unstable to antiferromagnetism and it corresponds physically to a highly frustrated system. The analysis of the spectral function along the two solutions (allowing and forbidding magnetic ordering, Fig. 2) reveals that the transition takes place also in the absence of antiferromagnetism. Namely, at small V , a phase with no spectral weight at the Fermi level is realized in both cases. The Kondo peak present in the PM phase disappears in going across the transition, leaving behind a pseudogap, and the f electrons effectively decouple from the conduction band, at least within the energy resolution of our calculations. The transition is an orbitally selective Mott transition for the f band. This implies that the f electrons do not contribute to the Fermi surface for $V < V^*$. This is in marked contrast with the paramagnetic single-site DMFT solution where there is only a Fermi liquid Kondo

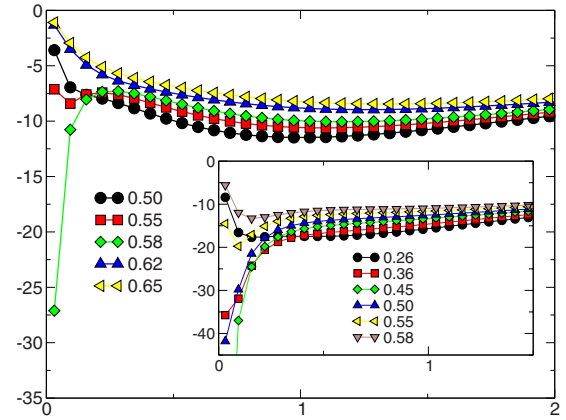


FIG. 3. (Color online) Imaginary part of the even self-energy eigenvalue on the imaginary axis for different values of the hybridization. Inset: odd eigenvalue (in a different range of hybridization values).

screened phase and no sign of such a transition or of a pseudogapped phase. Notice also that in the CDMFT treatment the f transfer of spectral weight takes place from the Fermi level to its immediate vicinity as the hybridization is reduced. This should be contrasted with the single-site DMFT description of the Mott transition in the Hubbard model where the spectral weight is transferred from the Fermi level directly to the Hubbard bands at much higher energies.

To clarify the Mott character of the transition we plot in Fig. 3 the imaginary frequency behavior of the two $\hat{\Sigma}$ eigenvalues within the PM solution, named, respectively, $\hat{\Sigma}_{even} = \hat{\Sigma}_{11} + \hat{\Sigma}_{12}$ and $\hat{\Sigma}_{odd} = \hat{\Sigma}_{11} - \hat{\Sigma}_{12}$. Approaching the transition from the PM phase the slope at zero frequency of both eigenvalues increases, signaling the growth of the effective mass in the Fermi liquid. At the transition the even eigenvalue develops a divergence signaling the end of the Fermi liquid description and the beginning of the Mott insulating phase. The odd eigenvalue has a similar divergence at a lower value of the hybridization as shown in the inset. A qualitative understanding of this behavior can be proposed considering that $\hat{\Sigma}_{even}$ and $\hat{\Sigma}_{odd}$ represent in a loose sense the lattice self-energy calculated around momenta $(0,0,0)$ and (π, π, π) , respectively. Hence the Mott transition corresponds to the first appearance of a surface poles in the self-energy around the origin of the Brillouin zone. Decreasing further the hybridization the surface of poles moves toward the corner of the zone and finally disappears for $V \sim 0.43$.

While for $V > V^*$ the self-energy was approximately local, in the PM solution the development of magnetism for $V < V^*$ is replaced by a dramatic increase of nonlocal correlations as shown in Fig. 4, where we plot the real part of $\hat{\Sigma}_{12}$ at the lowest available frequency in the imaginary axis.

The behavior of T_K , of the spectral function, and of the off-diagonal self-energy near the transition is very similar to the corresponding behavior found in the 2IKM close to its QCP.^{31–33} To establish this connection we used Wilson's numerical renormalization group to solve the impurity model underlying the self-consistency in the PM case for the same set of parameters. The difference with the ED calculation is

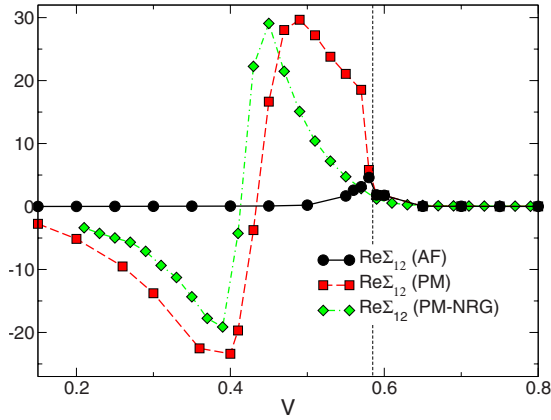


FIG. 4. (Color online) Nonlocal correlations ($\text{Re } \Sigma_{12}$, calculated at the lowest available imaginary frequency) along the AF and PM solutions. The vertical dashed line marks the transition. For comparison with the PM case the NRG results (without self-consistency).

that we used a constant density of states for the NRG bath, so the results are non-self-consistent. The results are nevertheless qualitatively similar. The main difference between the results of the two calculations is that the transition found in CDMFT is replaced in NRG by a crossover. We ascribe this effect to the lack of a self-consistent bath in the NRG calculation. In Fig. 4 we compare the nonlocal correlations, finding a very good agreement. Other features such as the pseudogap formation around V^* are also reproduced. The similarity of these two results suggests that most of the physics relevant to the lattice is already captured at the level of the two-impurity problem. In this case the onset of magnetism in the lattice model can be understood as arising from the vicinity to the impurity QCP. Indeed at the 2IKM critical point there are three relevant operators that correspond to possible symmetry breaking instabilities. Susceptibilities in the antiferromagnetic, superconducting, and p - h symmetry breaking channels are diverging at the impurity QCP. Since p - h symmetry is already broken in the lattice system, only the other two instabilities are left to provide a way to quench the residual entropy associated with the QCP. In this work we did not consider the superconducting instability but we expect it to play a relevant role (and possibly compete with antiferromagnetism) depending on the specific details of the band structure of the realistic material.

Notice, however, several important differences with the picture of local quantum criticality of Ref. 20. The reference system describing the physics of the lattice model requires a cluster of two sites, rather than one, embedded in a medium. The critical point of this two-impurity model has two relevant directions corresponding to varying the hybridization and breaking p - h symmetry. So the impurity model without the self-consistency condition has a multicritical point rather than a critical point. Generic problems, as the one considered in this paper, are p - h asymmetric, and therefore in these cases the two-impurity QCP is not reachable. However, the analysis of the NRG low-energy spectrum confirms that in going from one side to the other of the crossover (correspondingly, from one side to the other of the transition in the

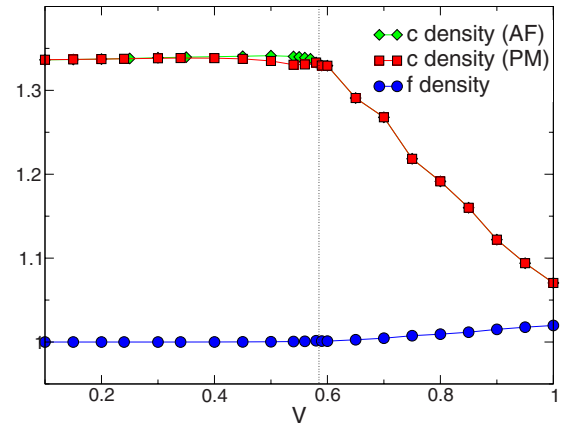


FIG. 5. (Color online) f and c electron occupation per site. The transition is marked by the vertical dashed line.

CDMFT case) the system evolves from a state in which the impurities are screened by the conduction electrons (for large V) to a state in which the impurities take advantage of the RKKY interaction to form a singlet and decouple from the conduction band (for small V). Hence the low-energy picture for $V < V^*$ is that of a conduction band asymptotically decoupled from a collection of spins arranged in singlets. In the lattice model the self-consistency condition transforms the crossover of the impurity model into a true phase transition.

Following the paramagnetic solution we can also observe a violation of the Luttinger theorem for $V < V^*$ in the form of a mismatch between the number of particles and the volume of the Fermi surface. This is clear from the plot of the number of c and f electrons per site as a function of V (Fig. 5). In the PM phase both the conduction and the f bands are doped ($n_f, n_c \neq 1$). In this case the Fermi surface has a volume equal to the doping $\delta = n_c + n_f - 2$. The total occupation is not constant because we fixed the chemical potential rather than the density. For $V < V^*$ the occupation in both bands becomes essentially constant, implying that V is no more effective. In this regime the only contribution to the Fermi surface comes from the c electrons which, being noninteracting and decoupled from the f band, have a Fermi surface with volume $n_c = 1 + \delta$. These results once again support the orbitally selective Mott transition picture of the KB,^{12,13} namely, an f -like fluid that becomes incompressible beyond the KB point.

In Fig. 6 we plot the k -resolved total spectral density $-\frac{1}{\pi} \text{Im}[G_c(\mathbf{k}, \omega) + G_f(\mathbf{k}, \omega)]$ at low energies along the paramagnetic solution in the two phases. We intentionally consider points far from the transition to show that the results are robust and do not depend on the vicinity to special points in the phase diagram. To obtain this quantity we reconstruct the rotational and translational lattice symmetries, broken by the cluster-tiling procedure, by periodization of the cumulants.³⁴ This scheme is more appropriate when correlations are stronger. Indeed the simple periodization of the self-energy does not reproduce the local quantities correctly upon integration over momenta, introducing spurious states in gapped regions of the spectrum. In panel (a) the system is in the PM phase ($V=0.65$). It is possible to track the origin of the small value of Z in the narrow band crossing the chemi-

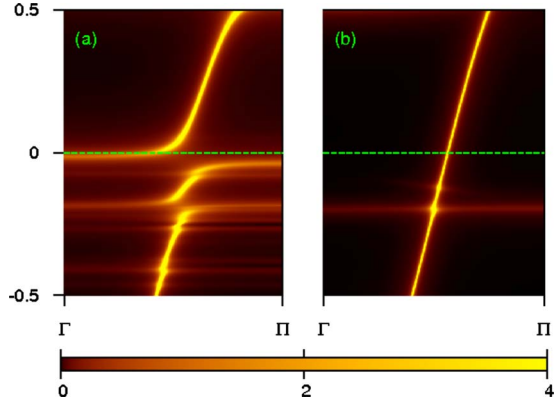


FIG. 6. (Color online) Total spectral function as a function of momentum and energy on the path connecting the origin $\Gamma = (0,0,0)$ and the corner $\Pi = (\pi, \pi, \pi)$ of the Brillouin zone. (a) $V = 0.65$ PM phase. (b) $V = 0.30$ PM solution in the AF phase.

cal potential. The Fermi surface encloses a “small” region of the Brillouin zone centered around the origin. In panel (b) we show the PM solution in the AF phase ($V = 0.30$). It is clear that the volume of the Fermi surface in this phase has increased. The difference between the Fermi surface volume and the density is equal to one within the numerical precision, confirming the violation of the Luttinger theorem as expected in the orbital-selective Mott transition.¹³ It is also possible to track the nondispersive f band at around $\omega \sim -0.2$.

Since the PM solution for $V < V^*$ is unstable to antiferromagnetism, to make contacts with experiments we plot in Fig. 7 the spectral density for the AF solution ($V = 0.50$). The bands are doubled because of the AF ordering. These results are representative for the whole AF phase down to small value of V . The striking difference with respect to the PM phase is the big rearrangement of the spectral weight: now the occupied region is centered around the $(\frac{\pi}{2}, \frac{\pi}{2}, \frac{\pi}{2})$ point. This result implies a sudden jump across the antiferromagnetic transition in all the properties connected with the topology of the Fermi surface and it is consistent with the experi-

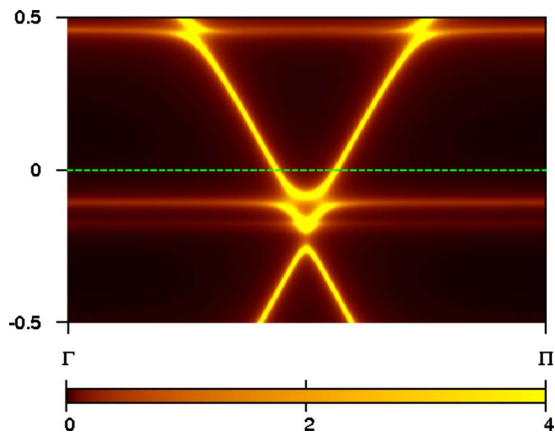


FIG. 7. (Color online) Total spectral function as a function of momentum and energy along the same path of Fig. 6 for the AF solution ($V = 0.50$).

mental observation of a discontinuous behavior of the Hall coefficient³⁵ and of the de Haas–van Alphen frequencies.³⁶ The contribution of the f electrons in this phase is manifest in the two nondispersing bands at $\omega \sim -0.1$ and $\omega \sim 0.45$, corresponding to the two peaks in Fig. 2, while the bands crossing the chemical potential have mostly c character.

IV. CONCLUSIONS

To summarize, we have constructed and investigated a cluster dynamical mean-field theory for the periodic Anderson model using a link as a reference frame to capture the competition of the Kondo effect and the RKKY interaction. The mean-field phase diagram away from half-filling features a transition separating a paramagnetic heavy electron phase from an antiferromagnetic phase. In the PM phase, the phase transition is accompanied by a strong renormalization of quasiparticles, marked by a large enhancement of the effective mass on all the Fermi surface.

By constraining a mean-field metastable paramagnetic solution into the AF region of the phase diagram, we have been able to show that the transition can be described as an orbitally selective Mott transition. The decoupling of the f band from the conduction band marks a localization of the f electrons, as shown by the opening of a pseudogap in the single particle spectrum and the appearance of poles in the self-energy at the Fermi level, a clear fingerprint of “Mottness.” This is further supported by the incompressibility of the system, which presents a constant density by varying the hybridization, and by the violation of the Luttinger theorem for $V < V^*$ along the PM solution. It is important to compare this transition, which presents an orbital-selective Mott character, with the traditional DMFT Mott transition of the single band Hubbard model. In the present case the weight is shifted from the chemical potential to the immediate vicinity forming a pseudogap rather than being transferred to the Hubbard bands at much higher energy. This feature is the product of our link-DMFT analysis in three dimensions, strikingly different from the infinite dimensional DMFT result where the physics is purely local. It would be important in future DMFT investigations to better understand the nature of this Mott-like transition by studying its cluster-size dependence.

In the SDW scenario, the fermions which are not coupled by the ordering vector are unaffected by the transition. On the contrary in our CDMFT study, the transition is accompanied by a dramatic rearrangement of the Fermi surface, in agreement with recent experiments.^{35,36}

Our findings can be understood in terms of proximity to a decoupling QCP with the same properties of the QCP found in the 2IKM, namely, the impurity model underlying the self-consistency equations. Although the lattice system cannot reach that critical point due to the particle-hole symmetry breaking, the region in which the effect of the critical point is relevant is large enough to trigger the lattice antiferromagnetic instability.³¹ If we follow the paramagnetic solution the vicinity to the critical point results instead in an increase of the nonlocal correlations Σ_{12} in agreement with the behavior of the 2IKM. In real systems this effect is preempted by the lattice antiferromagnetic instability. It would be interesting to

realize heavy fermion systems in highly frustrated lattices to suppress the antiferromagnetic instability. This would provide a physical realization of the paramagnetic solution of the CDMFT equations.

In this framework the antiferromagnetic transition is the result of the response of the system to the instability of the nearby decoupling QCP, rather than being an intrinsic feature. Notice that other correlations are diverging at the 2IKM critical point. We expect that depending on the details of the model other instabilities (mainly superconductivity) compete with antiferromagnetism to order the system and quench the residual entropy of the unstable QCP.

We believe that our description captures the correct physics of the periodic Anderson model in an intermediate asymptotic regime of energies and proximity to the transition. At higher energies, the single-site DMFT description is regained. At very low energies and very close to the transi-

tion, further nonlocal effects could turn out to be very important. We do not know if our treatment fits within the local quantum criticality paradigm where no spatial anomalous dimensions are generated. To elucidate these questions would require the investigation of the dynamical susceptibility beyond the cluster DMFT approximation, which is beyond the scope of this work.

ACKNOWLEDGMENTS

We would like to thank M. Fabrizio, A. Georges, F. Steglich, P. Coleman, C. Pepin, I. Paul, O. Parcollet, P. Sun, K. Haule, E. Lebanon, M. Capone, T. Stanescu, J. C. Domenge, and L. de' Medici for helpful discussions and comments. This work was supported by the NSF under Grant No. DMR 0528969. L.D. and G.K. gratefully acknowledge support by the International ICAM Junior Exchange Award Program.

-
- ¹G. R. Stewart, *Rev. Mod. Phys.* **73**, 797 (2001).
²J. A. Hertz, *Phys. Rev. B* **14**, 1165 (1976).
³A. J. Millis, *Phys. Rev. B* **48**, 7183 (1993).
⁴T. Moriya and T. Takimoto, *J. Phys. Soc. Jpn.* **64**, 960 (1995).
⁵A. Schroeder, G. Aeppli, R. Coldea, M. Adams, O. Stockert, H. V. Loehneysen, E. Bucher, R. Ramazashvili, and P. Coleman, *Nature (London)* **407**, 351 (2000).
⁶P. Gegenwart, J. Custers, C. Geibel, K. Neumaier, T. Tayama, K. Tenya, O. Trovarelli, and F. Steglich, *Phys. Rev. Lett.* **89**, 056402 (2002).
⁷J. Custers, P. Gegenwart, H. Wilhelm, K. Neumaier, Y. Tokiwa, O. Trovarelli, C. Geibel, F. Steglich, C. Pepin, and P. Coleman, *Nature (London)* **424**, 524 (2003).
⁸P. Coleman, C. Pepin, Q. Si, and R. Ramazashvili, *J. Phys.: Condens. Matter* **13**, R723 (2001).
⁹S. Nakatsuji, D. Pines, and Z. Fisk, *Phys. Rev. Lett.* **92**, 016401 (2004).
¹⁰P. Sun and G. Kotliar, *Phys. Rev. Lett.* **95**, 016402 (2005).
¹¹S. Doniach, *Physica B & C* **91**, 231 (1977).
¹²L. de' Medici, A. Georges, G. Kotliar, and S. Biermann, *Phys. Rev. Lett.* **95**, 066402 (2005).
¹³C. Pepin, *Phys. Rev. Lett.* **98**, 206401 (2007).
¹⁴T. Senthil, M. Vojta, and S. Sachdev, *Phys. Rev. B* **69**, 035111 (2004).
¹⁵S. Burdin, D. R. Grempel, and A. Georges, *Phys. Rev. B* **66**, 045111 (2002).
¹⁶N. Andrei and P. Coleman, *Phys. Rev. Lett.* **62**, 595 (1989).
¹⁷C. Castellani, M. Grilli, and G. Kotliar, *Phys. Rev. B* **43**, 8000 (1991).
¹⁸P. Sun and G. Kotliar, *Phys. Rev. Lett.* **91**, 037209 (2003).
¹⁹P. Sun and G. Kotliar, *Phys. Rev. B* **71**, 245104 (2005).
²⁰Q. Si, S. Rabello, K. Ingersent, and J. L. Smith, *Nature (London)* **413**, 804 (2001).
²¹D. R. Grempel and Q. Si, *Phys. Rev. Lett.* **91**, 026401 (2003).
²²J.-X. Zhu, D. R. Grempel, and Q. Si, *Phys. Rev. Lett.* **91**, 156404 (2003).
²³J.-X. Zhu, S. Kirchner, R. Bulla, and Q. Si, *Phys. Rev. Lett.* **99**, 227204 (2007).
²⁴M. T. Glossop and K. Ingersent, *Phys. Rev. Lett.* **99**, 227203 (2007).
²⁵Q. Si, J.-X. Zhu, and D. R. Grempel, *J. Phys.: Condens. Matter* **17**, R1025 (2005).
²⁶I. Paul, C. Pepin, and M. R. Norman, *Phys. Rev. Lett.* **98**, 026402 (2007).
²⁷G. Kotliar, S. Y. Savrasov, G. Pálsson, and G. Biroli, *Phys. Rev. Lett.* **87**, 186401 (2001).
²⁸M. Caffarel and W. Krauth, *Phys. Rev. Lett.* **72**, 1545 (1994).
²⁹B. A. Jones, C. M. Varma, and J. W. Wilkins, *Phys. Rev. Lett.* **61**, 125 (1988).
³⁰I. Affleck, A. W. W. Ludwig, and B. A. Jones, *Phys. Rev. B* **52**, 9528 (1995).
³¹L. De Leo and M. Fabrizio, *Phys. Rev. B* **69**, 245114 (2004).
³²L. Zhu and C. M. Varma, arXiv:cond-mat/0607426.
³³M. Ferrero, L. De Leo, P. Lecheminant, and M. Fabrizio, *J. Phys.: Condens. Matter* **19**, 433201 (2007).
³⁴T. D. Stanescu, M. Civelli, K. Haule, and G. Kotliar, *Ann. Phys.* **321**, 1682 (2006).
³⁵S. Paschen, T. Luhmann, S. Wirth, P. Gegenwart, O. Trovarelli, C. Geibel, F. Steglich, P. Coleman, and Q. Si, *Nature (London)* **432**, 881 (2004).
³⁶H. Shishido, R. Settai, H. Harima, and Y. Onuki, *J. Phys. Soc. Jpn.* **74**, 1103 (2005).